Lawrence Berkeley National Laboratory

Lawrence Berkeley National Laboratory

Title

The adsorption of water on Cu2O and Al2O3 thin films

Permalink

https://escholarship.org/uc/item/90c056tw

Author

Deng, Xingyi

Publication Date

2008-07-03

Peer reviewed

eScholarship.org Powered by the California Digital Library
University of California

The adsorption of water on Cu_2O and Al_2O_3 thin films

Xingyi Deng[1], Tirma Herranz[1], Christoph Weis[1], Hendrik Bluhm[2] and Miquel Salmeron[1,3]

[1]Materials Sciences Division, Lawrence Berkeley National Laboratory

[2]Chemical Sciences Division, Lawrence Berkeley National Laboratory

[3]Materials Science and Engineering Department, University of California, Berkeley, CA 94720, USA

E-mail: MBSalmeron@lbl.gov

RECEIVED DATE (to be automatically inserted after your manuscript is accepted if required according to the journal that you are submitting your paper to)

*Author to whom correspondence should be addressed.

Abstract

The initial stages of water condensation, approximately 6 molecular layers, on two oxide surfaces, Cu_2O and Al_2O_3, have been investigated using ambient pressure x-ray photoelectron spectroscopy at relative humidity values (RH) from 0 to > 90%. Water adsorbs first dissociatively on oxygen vacancies producing adsorbed hydroxyl groups in a stoichiometric reaction: O_{lattic} + Vacancies + H_2O = 2OH. The reaction is completed at ~ 1% RH and is followed by adsorption of molecular water. The thickness of the water film grows with increasing RH. The first monolayer is completed at ~ 15% RH on both oxides and is followed by a second layer at 35-40% RH. At 90% RH, about 6 layers of H_2O film have been formed on Al_2O_3.

Keywords: wetting, oxides, Cu_2O, Al_2O_3, H_2O, adsorbed hydroxyl, ambient pressure x-ray photoelectron spectroscopy.

Introduction

The study of water at interfaces is an active field which is motivated by the desire to understand many important processes involving water, such as corrosion, catalysis, environmental chemistry, and biological processes. Oxides are among the most relevant materials in many processes and thus have received considerable attention. For example, oxides constitute many of the natural rock minerals existing on the earth. They are also widely used in catalysis as supports, promoters, additives and as catalysts. Therefore, the interactions between water and oxides have been extensively studied and reviewed.[1-4] Surface science studies in ultrahigh vacuum (UHV) and at low temperatures have provided detailed information of the interactions at a molecular level,[1,2] one of the main focus being molecular *vs.* dissociative adsorption in the first monolayer, as this might determine the structure and subsequent growth characteristics of the films.

The presence of wetting layers of water on oxides is assumed to be ubiquitous under ambient conditions. However, molecular scale investigations of the processes leading to wetting are rarely carried out. Questions regarding the structure of the first water layer in contact with the surface and the thickness of the water film under typical relative humidity (RH) conditions are waiting to be answered. Recently, investigations under near ambient conditions using near edge x-ray adsorption fine structure (NEXAFS)[5] and x-ray photoelectron spectroscopy (XPS)[5,6] have successfully addressed adsorption of water on oxides in equilibrium with the vapor. On SiO_2, NEXAFS acquired at ~ 70% RH revealed that the local electronic structure of the adsorbed water molecules in films as thin as 4-5 monolayers is similar to that of the bulk liquid above 0 ^oC, and to that of ice below that temperature.[5] On the single crystal TiO_2(110) surface Ketteler *et al.* quantified the amount of adsorbed water as function of RH and showed the important role played by surface OH in the nucleation of water based on the ambient pressure XPS results.[6]

In this paper we present the results of an ambient pressure XPS study of two thin polycrystalline oxide films, Cu_2O and Al_2O_3, in the presence of water vapor at near ambient conditions. Cu_2O is a p-type semiconductor (band gap (Δ) ~ 2.0-2.2 eV[7]) that attracts much attention due to its potential for application in solar energy converting devices.[8-10] Copper is also used as electrical conductor in electronic microcircuits and as an electrode material in electrical motors. When exposed to air its surface is covered by an oxide.[11] Al_2O_3 is a wide band gap oxide (Δ = 8.8 eV[12]) used as insulating material in electronic devices and also as a support in catalysis. We conducted systematic experiments on these two surfaces to investigate their wetting characteristics. In both cases initial dissociation of H_2O to OH, presumably at defect sites, was observed. This is followed by the growth of molecular water films with a thickness that was determined as a function of RH. The molecular scale wetting mechanism is discussed based on these findings.

Experimental

Surface preparation

Preparation of the Cu_2O surface was carried out by oxidation of a copper foil *in-situ*. Prior to oxidation the pure polycrystalline Cu foil (99.999% from Alfa Aesar) was cleaned by several cycles of sputtering with Ar^+ ions (10^{-5} torr, 1.5 keV) for 30 minutes, followed by heating to 800 K for 5 minutes. The clean surface was then exposed to 3×10^{-2} torr O_2 at 430 K for 30 minutes. After that treatment XPS showed a valence band shape characteristic of an oxide with a band edge 0.9 eV below the Fermi level.[13,14] The thickness of the oxide overlayer was estimated to be $\geq$ 1.5 nm based on the depth profiling by variation of the incident photon energy.

For Al_2O_3 the native film formed in air on a pure polycrystalline Al foil (99.999% from Alfa Aesar) was used. The main contaminants on the surface were hydrocarbon species (CH_x), which were removed by sputtering with Ar^+ ions (10^{-5} torr, 1.0 keV) for 30 minutes. The Al_2O_3 film was characterized by an Al *2p* peak at a binding energy (BE) of 75.7 eV and an O *1s* peak at a BE of 532.8 eV in XPS. The original thickness of the oxide layer was estimated to be 4.4 ± 0.1 nm using a

calibration method similar to that of Himpsel et al.,[15] with the error indicating statistical dispersion. A slight decrease of the thickness of the oxide layer (<0.7 nm) due to the Ar^+ ion sputtering was observed.

XPS experiments

All XPS measurements were performed using a specially designed photoemission spectrometer that can operate at near-ambient pressures (several Torr) located at the undulator beamline 11.0.2. of the Advanced Light Source (Berkeley, USA).[16,17] The O *1s* XP spectra were recorded at photon energies of 735 eV, corresponding to a photoelectron kinetic energy of 200 eV. To ensure the same probing depth in all spectral regions, the Cu *3p* and Al *2p* spectra were recorded at photon energies of 310 and 285 eV respectively, i.e. with the same photoelectron kinetic energy of 200 eV.

The relative humidity (RH) during the XPS measurements was controlled by varying the vapor pressure and/or sample temperature. The RH is defined as $p/p_v(T) \times 100$, where p_v is the equilibrium vapor pressure of bulk water or ice at the corresponding temperature. For studies on Al_2O_3, a RH of higher than 90% could be achieved by lowering the surface temperature to 260 K at a water pressure of 1.5 torr using a sample holder with a Peltier element. However, this holder does not permit heating the sample to temperatures higher than 350 K and thus could not be used for experiments on Cu_2O, which require heating to prepare the surface. In those experiments a stainless steel sample holder with a ceramic button heater was used. The maximum RH there was limited in this case to ~ 40%.[18]

The XPS data analysis was analyzed using non-linear (Shirley) background subtraction and curve fitting with mixed Gaussian-Lorentzian functions. For studies on Cu_2O, the fitted peaks were constrained at positions known from the literature but with independent and variable full width at half maximum (FWHM, 0.9-1.1 eV) and intensities. In case of Al_2O_3, the peak parameters, such as the percentage of Gaussian function (> 90%) and FWHM (2.1-2.4 eV), were first determined using the O *1s* spectrum recorded in UHV (a single peak due to Al_2O_3). Then these peak parameters were constrained during the curve fitting process but with independent and variable positions and intensities as optimized by the program.

Results

Cu_2O surface in the presence of H_2O

The O *1s* XPS spectrum of the as-prepared Cu_2O surface in UHV ($P < 1 \times 10^{-9}$ torr) is shown in Figure 1. The spectrum can be deconvoluted into a major peak at 530.2 eV BE, assigned to the lattice oxygen of Cu_2O, and a small peak (~ 5%) at 528.9 eV, assigned to an unknown species of oxygen. This small, unknown oxygen species persists in all experiments (< 5%) and has little influence on the results presented here.

A new oxygen species with a BE of 530.9 eV was observed when the sample was exposed to 1×10^{-7} torr of H_2O at 295 K (corresponding to a relative humidity of 5×10^{-7} %), as shown in Figure 1. The intensity of this peak increased rapidly with increasing RH up to ~1%. By comparison with the literature[19] we assign this species to OH (adsorbed hydroxyl). Other species already observed in UHV, i.e., the lattice oxygen (BE = 530.2 eV) and the unknown species of oxygen (BE = 529.1 eV), remained on the surface.

At ~1% RH, molecularly adsorbed H_2O (BE = 532.6 eV) was detected, as shown in Figure 1. The molecular H_2O peak grew with increasing RH and became the majority species at 35% RH. The lattice oxygen peak remained at BE = 530.2 eV, while the OH peak BE shifted by +0.2 eV to 531.1 eV. A similar OH BE shift was observed in a recent study of H_2O on Cu(110)[20] where the BE of OH shifted from 530.45 eV (for pure OH) to 530.8-531.0 eV (OH bound to H_2O).

It should be noted that at water pressures higher than 0.05 torr a peak due to gas phase H_2O is observed at BE = 535.0 eV.

The normalized intensities $I_{\text{lattice oxygen}}$ and I_{OH},[21] from XPS (O *1s* region) in the presence of H_2O at pressures $< 1 \times 10^{-5}$ torr are shown in Figure 2. At these pressures the scattering of the photoelectrons by the gas phase H_2O molecules is negligible, so that the population of oxygen species on the surface is directly proportional to their XPS peak intensity. As shown in Figure 2, the OH population increases at the expense of lattice oxygen. We also find that $I_{\text{lattice oxygen}} + \frac{1}{2} I_{OH} \approx$ constant. This observation is in an

agreement with the model proposed in the literature[1,2,6,22-25] where OH is formed by a stoichiometric reaction involving O-defect vacancies at the surface: H_2O + Vacancy + $O_{lattice}$ = 2OH.

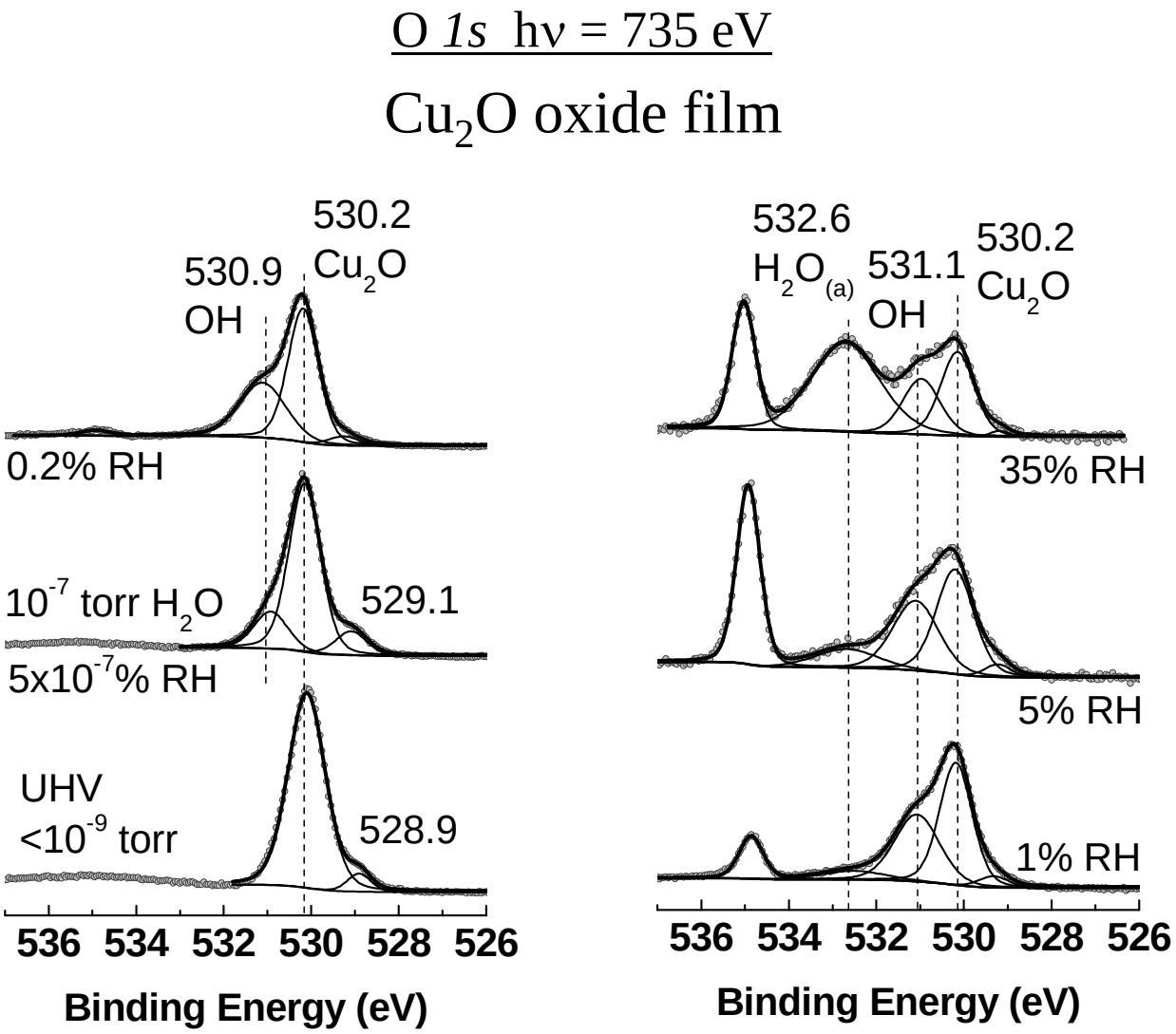

Figure 1. O *1s* XPS spectra of Cu_2O in UHV and at selected relative humidity (RH), showing the presence of various oxygen species, including lattice oxygen of Cu_2O, OH (adsorbed hydroxyl) and molecular adsorbed H_2O, on the surface. A sharp peak at higher BE at ~535 eV due to gas phase H_2O is also visible in the spectra at water pressures higher than 0.05 torr. The Cu_2O, with a thickness ≥ 1.5 nm, was prepared by *in-situ* oxidation of a Cu foil.

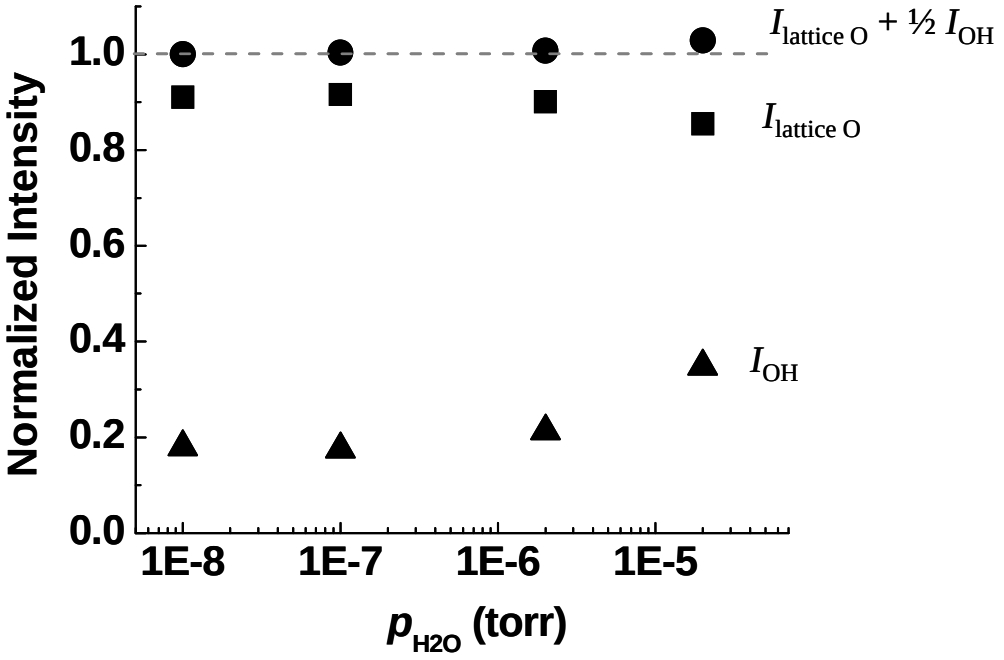

Figure 2. $I_{\text{lattice oxygen}}$ (solid squares) and I_{OH} (solid triangles) normalized from O *1s* XPS spectra of Cu_2O in the presence of H_2O at pressures < 1 × 10^{-5} torr,[21] and the values of corresponding $I_{\text{lattice oxygen}}$ + ½ I_{OH} (solid circles). The Cu_2O, with a thickness ≥ 1.5 nm, was prepared by *in-situ* oxidation of a Cu foil.

The ratio of OH to lattice oxygen and the thickness of the adsorbed H_2O layer on Cu_2O (see supporting information for detailed estimation method) as a function of the relative humidity are shown in Figure 3. Hydroxyls formed readily on Cu_2O even at very low RH (5 ×10^{-7} %), reaching saturation at ~ 1% RH. This result is similar to that obtained in the study of H_2O adsorption on TiO_2(110).[6] Molecularly adsorbed H_2O appeared at ~ 1% RH and grew monotonically with increasing RH, reaching a monolayer (assuming 3 Å per layer) at ~15% RH and two layers (or 6 Å thickness) at ~35% RH.

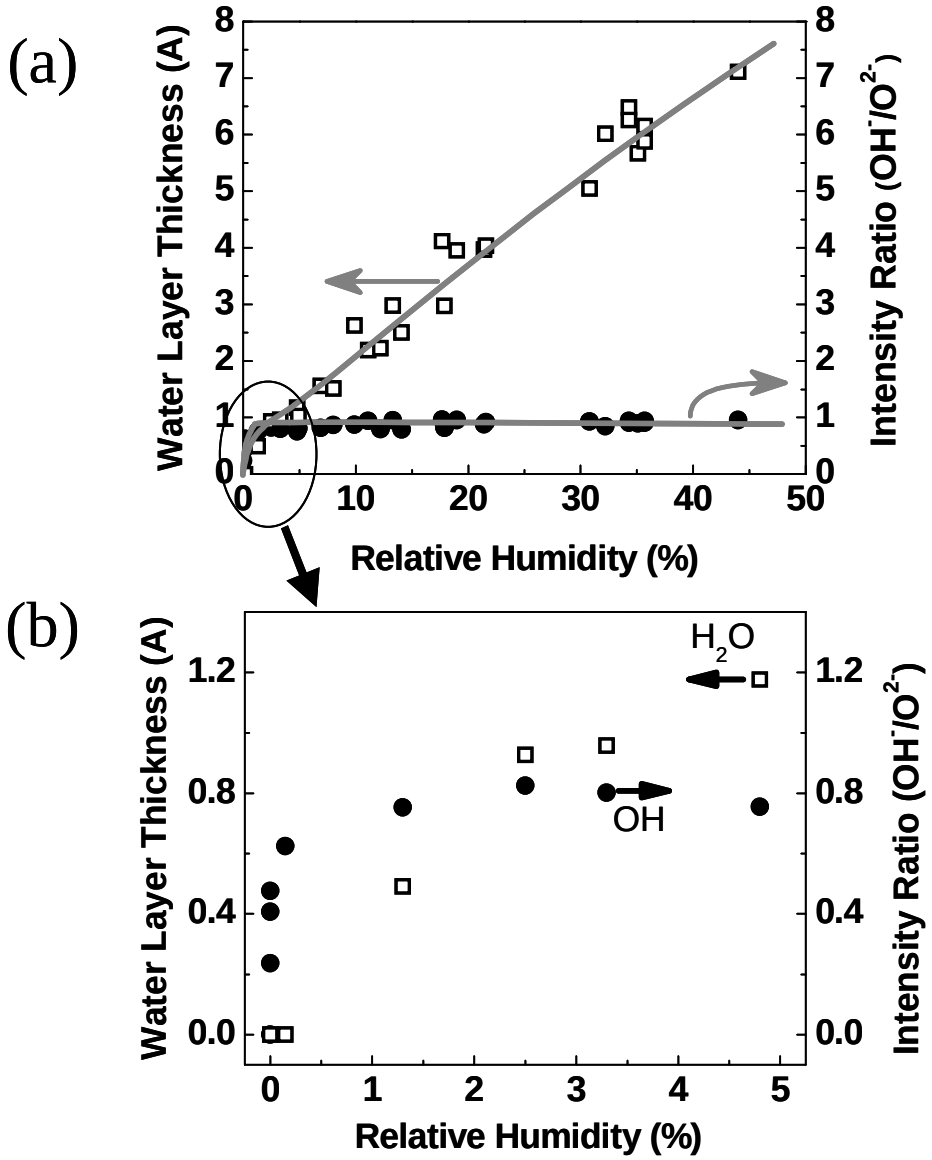

Figure 3. (a) Ratio of OH to lattice oxygen and the thickness of the adsorbed H_2O layer on Cu_2O as a function of relative humidity. (b) Enlarged view of the low relative humidity region. The Cu_2O, with a thickness ≥ 1.5 nm, was prepared by *in-situ* oxidation of a Cu foil.

Al_2O_3 surface in the presence of H_2O

A single peak (BE = 532.8 eV) was present in the O *1s* XPS spectrum of the as-prepared Al_2O_3 surface in UHV (Figure 4). We assign this peak to the lattice oxygen of Al_2O_3. The full width at half maximum (FWHM) of the peak was 2.2 eV, about twice larger than the O *1s* peak in Cu_2O, which was about 1 eV. We attribute the large width of the peak, at least in part, to inhomogeneous charging effects (photoelectrons and secondary electrons). This is likely due to the large band gap of Al_2O_3 (Δ = 8.8 eV[12]) and its thickness of 4.4 ± 0.1 nm, which favor the presence of charge traps.

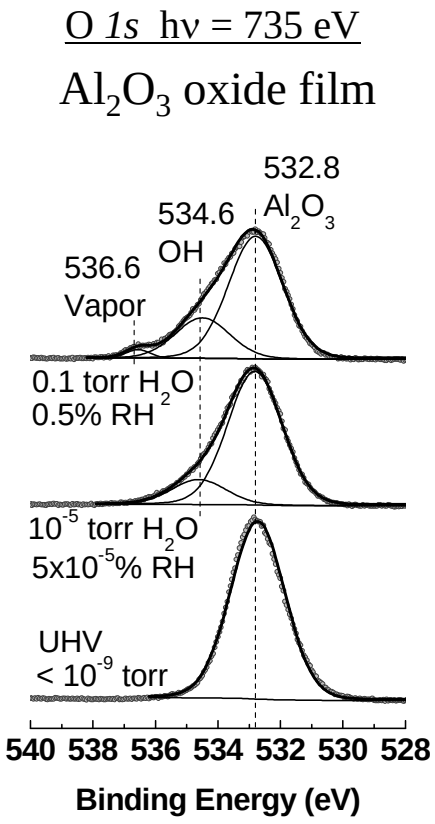

Figure 4. O *1s* XPS spectra of Al_2O_3 in UHV and at selected low relative humidity (RH), showing that OH is readily formed. The Al_2O_3, with a thickness of 4.4 ± 0.1 nm, was prepared by sputtering cleaning the native Al_2O_3 film formed in air on a pure polycrystalline Al foil.

As in the case of Cu_2O, OH was also produced readily on the Al_2O_3 surface at low RH. The hydroxyl O *1s* peak, with a BE of 534.6 eV, was visible when the sample was exposed to water vapor pressures higher than 1×10^{-5} torr H_2O at 295 K (corresponding to a relative humidity of 5×10^{-5} %), as

shown in Figure 4. The chemical shift between OH and the lattice oxygen is 1.8 eV, consistent with the value in the literature.[26]

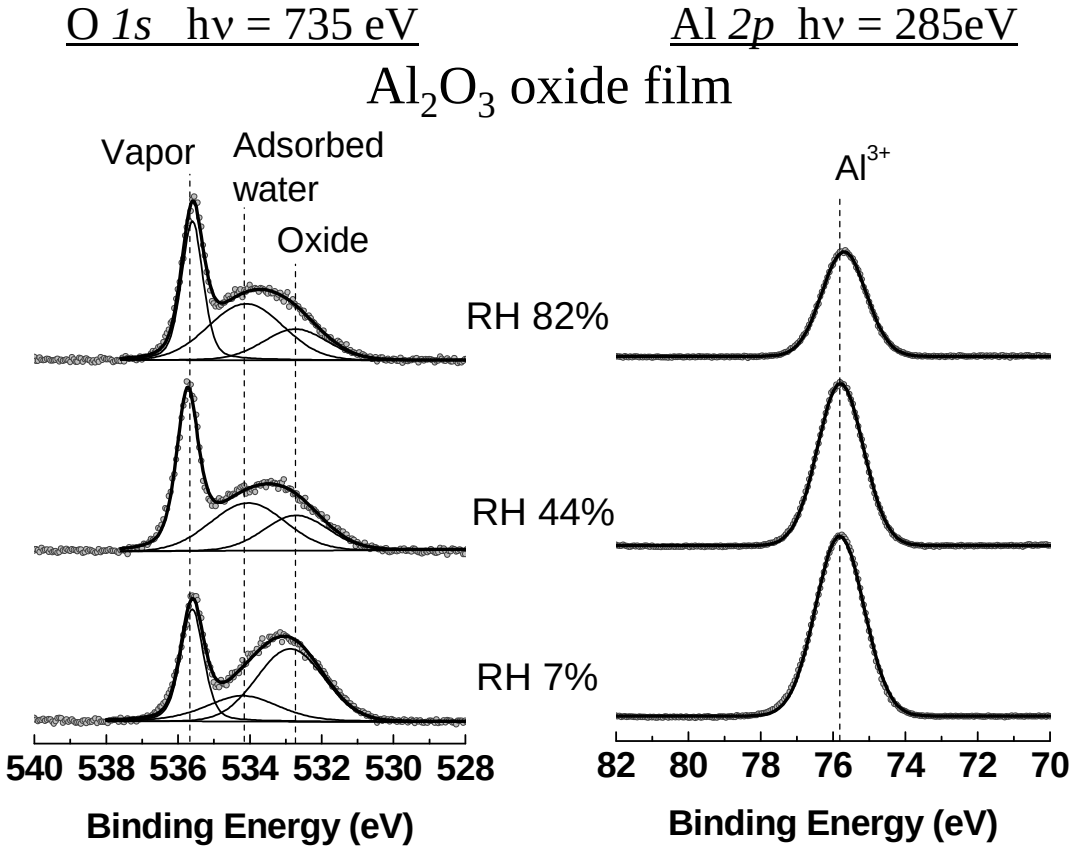

Figure 5. O *1s* and Al *2p* regions of the Al_2O_3 XPS spectra at selected RH values, showing the growth of a water film. In the O region, the adsorbed H_2O produces a peak at BE = 534.2 eV. In the Al region, the Al *2p* peak is progressively attenuated due to H_2O adsorption. Both O *1s* and Al *2p* peaks were normalized to the x-ray beam flux. The 4.4 ± 0.1 nm Al_2O_3 film was prepared by sputtering cleaning the native Al_2O_3 film formed in air on a pure polycrystalline Al foil.

Representative O *1s* and Al *2p* XPS spectra acquired at higher RH values are shown in Figure 5. In the O *1s* region, the XP spectra can be deconvoluted into three peaks at all RH: 532.8 eV, due to the lattice oxygen of Al_2O_3, 534.2 eV, assigned to adsorbed H_2O, and 535.7 eV, assigned to gas phase H_2O. Unfortunately, unlike the case in Cu_2O, when adsorbed molecular H_2O is present we could not resolve the OH peak from that of H_2O because the peaks are too broad and their BE are too close. The growth of

the H_2O overlayer with increasing RH produces an attenuation of the lattice oxygen and Al *2p* peak intensities.

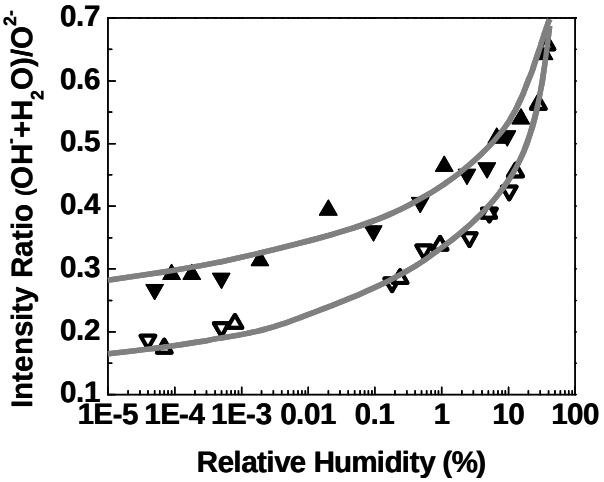

Figure 6. The ratios of $I_{OH + H2O}$ to $I_{lattice\ oxygen}$, quantified from the XPS data (O *1s* region), on a sputtered (solid symbols) and on an annealed Al_2O_3 (open symbols) as a function of RH. The sputtered Al_2O_3 surface was prepared by sputtering cleaning the native Al_2O_3 film formed in air on a pure polycrystalline Al foil, while the annealed surface was prepared by annealing the sputtered surface in O_2 (1×10^{-5} torr) at 800 K for 5 minutes followed by cooling in O_2 (1×10^{-5} torr).

Figure 6 shows the ratios of the integrated intensity under the OH+H_2O peaks near 535 eV ($I_{OH + H2O}$) and that under the lattice oxygen peak at 532.8 eV ($I_{lattice\ oxygen}$), on sputtered and on annealed Al_2O_3 as a function of RH. The sputtered surface was prepared as described in the experimental section, while the annealed surface was prepared by annealing the sputtered surface in O_2 (1×10^{-5} torr) at 800 K for 5 minutes followed by cooling in O_2 (1×10^{-5} torr). Although the OH and H_2O peaks cannot be deconvoluted due to their width and strong overlap, we assume that only OH is present at low RH (< 1%), based on the results of H_2O on Cu_2O. This assumption is consistent with the higher concentration of OH at low RH on the sputtered surface (solid symbols) as compared to the annealed one (open symbols). It suggests that, as in the case of Cu_2O, defect sites are crucial for dissociating H_2O to OH. The assumption of an exclusive presence of OH at low humidity followed, after saturation, by growth of

molecular water is supported by the fact that the $I_{OH + H2O}$ curves in figure 6 converge into the same curve at high RH, as it becomes dominated by molecularly adsorbed H_2O on both sputtered and annealed Al_2O_3 surfaces.

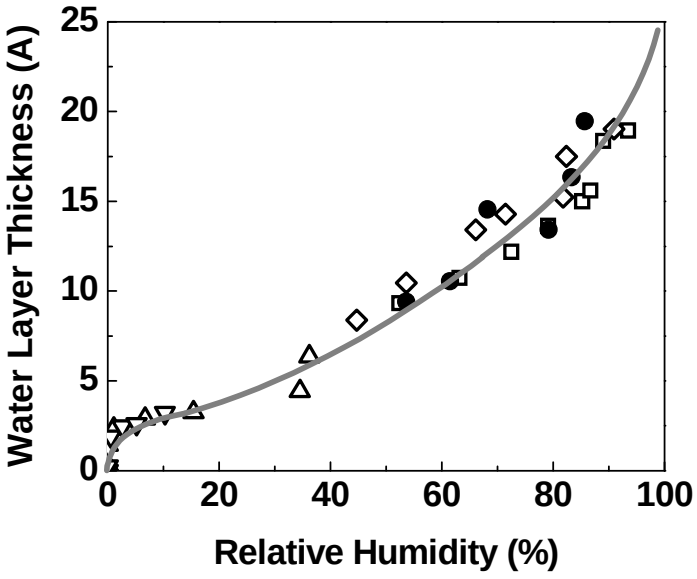

Figure 7. Thickness of the adsorbed OH + H_2O layer on Al_2O_3 as a function of relative humidity. Most of the growth is due to H_2O as OH saturates very early, at RH <1%. The open symbols indicate thickness values calculated from the O *1s* peak intensities (different open symbols correspond to experiments performed on different samples and/or at different background water vapor pressures), while the solid circles indicate values calculated from the attenuation of the Al *2p* peak by the water overlayer. The results from both calculations are in good agreement. The Al_2O_3, with a thickness of 4.4 ± 0.1 nm, was prepared by sputtering the native Al_2O_3 film formed in air on a pure polycrystalline Al foil.

The water overlayer thickness determined from the peak intensities as a function of RH is shown in Figure 7. The open symbols indicate thickness values calculated using the O *1s* peak intensities (different symbols correspond to experiments performed on different samples and/or at different background water vapor pressures). The solid circles indicate values calculated from the attenuation of the Al *2p* peak by the water overlayer. The results from both calculations are in good agreement. As seen

in Figure 7, the adsorbed H_2O formed a complete monolayer at ~15% RH. The second, third and fourth layers of H_2O were completed at 40%, 55%, and 70% RH, respectively. Above 70% RH, H_2O layers grew rapidly, reaching 18 Å (or approximately 6 layers) at 90% RH.

Discussion

The dissociation of H_2O on defective oxides, especially on TiO_2, has been investigated in detail in UHV,[1,2,6,22-25] where it was shown that a H_2O molecule dissociates readily at oxygen vacancy sites, resulting in the formation of two OH, one that fills the vacancy, the other by reaction of the released hydrogen atom with a neighboring oxygen. This mechanism fits our observations on Cu_2O and Al_2O_3 in the presence of low vapor pressures. Specifically, we found that $I_{\text{lattice oxygen}} + ½\, I_{OH} \approx$ constant (observed on Cu_2O), in agreement with the stoichiometry of the above reaction. In addition, the observed correlation between OH concentration and defect density observed on Al_2O_3 clearly indicates the essential role of defect sites in dissociating H_2O.

As shown in Figures 1 and 3, we did *not* observe molecularly adsorbed H_2O until OH saturates on Cu_2O. This may simply reflect the more reactive nature of the defect sites, where H_2O binds preferentially to react and produce OH. It may also imply that the formation of OH might be a crucial step in the wetting process of oxide surfaces. In fact, the observation that water desorbs at higher temperatures from a mixed OH+H_2O layer than from a pure H_2O layer on many metal surfaces, including Cu(110),[27,28] Ag(110),[29] Ni(110),[30] Pt(110),[31] Ru(0001),[32,33] and Rh(111),[34] suggests that the attractive interaction between H_2O and OH is stronger than between two intact water molecules.[19] Similarly, on TiO_2(110), the adsorption enthalpy of water is larger at very low coverage, when it coexists with OH species.[6]

The role of OH in the binding of water can be gleaned from the observed BE shifts accompanying the adsorption of molecular H_2O. As we have seen, the binding energy of OH shifts by +0.2 eV during the initial adsorption of molecular water. This indicates an interaction that disturbs the local electronic structure of OH in the direction of increasing its O *1s* binding energy. In a simplistic model this could

indicate that OH acts as an H acceptor forming HO···H-OH bonds. Calculations using *ab initio* codes however, such as DFT, are needed to verify this point. The formation of hydrogen bonds between lattice oxygen atoms at the surface and H_2O (Cu_2O···H-OH) is more difficult to assess because no BE shifts were observed for the lattice oxygen when molecular H_2O was adsorbed.

The above discussions lead to the following important question: is the ability of a surface to form OH groups essential to determine its hydrophilic character? Or more importantly, will a surface be hydrophobic if it is incapable of producing OH? A recent comparison of Cu(111) and Cu(110) under near ambient conditions using ambient pressure XPS[19] seems to support this hypothesis: it was shown that adsorption of H_2O does not occur on the (111) surface even in the presence of 1 Torr of water at room temperature, while it occurred readily on the (110) surface, where H_2O dissociated to produce OH. It would be very interesting to perform experiments on an oxide surface where O-vacancy defects were not present. This however is not trivial as it is very difficult to prepare stoichiometric surfaces with no vacancy defects in vacuum. As we have seen in the case of Al_2O_3, although heating the surface in O_2 decreases the amount of defects a non-negligible amount is still left on the surface. We are currently pursuing several strategies to substantially remove vacancies and test the hydrophobic or hydrophilic character of such a surface.

On the basis of the above results and discussions, we propose that wetting on defective oxides include the following sequential steps: 1) under low H_2O pressures (i.e., in vacuum), H_2O dissociates at defect sites forming two OH groups; 2) the OH coverage saturates rapidly, after which no further H_2O dissociation occurs; 3) formation of the first water layer via stronger H-bonding interactions with OH; 4) growth of subsequent H_2O layers until bulk liquid or ice is formed, depending on the surface temperature.

Conclusions

On Cu_2O and Al_2O_3, H_2O adsorbs dissociatively on O-vacancy defects sites at low relative humidity (RH), forming OH (adsorbed hydroxyl). The amount of OH is stoichiometrically correlated

with the number of defect sites on the surface (2 OH per site). On both oxide surfaces, OH formation saturates rapidly at ~1% RH beyond which molecular H_2O adsorption occurs without further H_2O dissociation. The thickness of the H_2O film grows with increasing RH reaching one layer (3 Å) at ~15% RH and two layers (6 Å) at 35-40% RH. At ~90% RH, the thickness of H_2O film on Al_2O_3 reaches 18 Å, corresponding to about six layers of H_2O.

Acknowledgements. This work was supported by the Director, Office of Science, Office of Biological and Environmental Research, under the Department of Energy Contract No. DE-AC02-05CH11231. T.H. acknowledges also the financial support from the Ramon Areces Foundation.

Supporting Information Available: The detailed description of calculating the thickness of the H_2O film on oxide surfaces from the XPS data. This material is available free of charge via the Internet at: http://pubs.acs.org.

References

(1) Thiel, P. A.; Madey, T. E. *Surf. Sci. Rep.* **1987**, *7*, 211-385.

(2) Henderson, M. A. *Surf. Sci. Rep.* **2002**, *46*, 5-308.

(3) Verdaguer, A.; Sacha, G. M.; Bluhm, H.; Salmeron, M. *Chem. Rev.* **2006**, *106*, 1478-1510.

(4) Kelber, J. A. *Surf. Sci. Rep.* **2007**, *62*, 271-303.

(5) Verdaguer, A.; Weis, C.; Oncins, G.; Ketteler, G.; Bluhm, H.; Salmeron, M. *Langmuir* **2007**, *23*, 9699-9703.

(6) Ketteler, G.; Yamamoto, S.; Bluhm, H.; Andersson, K.; Starr, D. E.; Ogletree, D. F.; Ogasawara, H.; Nilsson, A.; Salmeron, M. *J. Phys. Chem. C* **2007**, *111*, 8278-8282.

(7) Grozdanov, I. *Mater. Lett.* **1994**, *19*, 281-285.

(8) Nozik, A. J. *Ann. Rev. Phys. Chem.* **1978**, *29*, 189-222.

(9) Khan, K. A. *Appl. Energy* **2000**, *65*, 59-66.

(10) Yang, H. M.; Ouyang, J.; Tang, A. D.; Xiao, Y.; Li, X. W.; Dong, X. D.; Yu, Y. M. *Mater. Res. Bull.* **2006**, *41*, 1310-1318.

(11) Platzman, I.; Brener, R.; Haick, H.; Tannenbaum, R. *J. Phys. Chem. C* **2008**, *112*, 1101-1108.

(12) Xiong, K.; Robertson, J.; Clark, S. J. *J. Appl. Phys.* **2007**, *102*, 083710.

(13) Ghijsen, J.; Tjeng, L. H.; Vanelp, J.; Eskes, H.; Westerink, J.; Sawatzky, G. A.; Czyzyk, M. T. *Phys. Rev. B* **1988**, *38*, 11322-11330.

(14) Bluhm, H.; Havecker, M.; Knop-Gericke, A.; Kleimenov, E.; Schlogl, R.; Teschner, D.; Bukhtiyarov, V. I.; Ogletree, D. F.; Salmeron, M. *J. Phys. Chem. B* **2004**, *108*, 14340-14347.

(15) Himpsel, F. J.; McFeely, F. R.; Taleb-Ibrahimi, A.; Yarmoff, J. A.; Hollinger, G. *Phys. Rev. B* **1988**, *38*, 6084-6096.

(16) Ogletree, D. F.; Bluhm, H.; Lebedev, G.; Fadley, C. S.; Hussain, Z.; Salmeron, M. *Rev. Sci. Instr*. **2002**, *73*, 3872-3877.

(17) Bluhm, H.; Andersson, K.; Araki, T.; Benzerara, K.; Brown, G. E.; Dynes, J. J.; Ghosal, S.; Gilles, M. K.; Hansen, H. C.; Hemminger, J. C.; Hitchcock, A. P.; Ketteler, G.; Kilcoyne, A. L. D.; Kneedler, E.; Lawrence, J. R.; Leppard, G. G.; Majzlam, J.; Mun, B. S.; Myneni, S. C. B.; Nilsson, A.; Ogasawara, H.; Ogletree, D. F.; Pecher, K.; Salmeron, M.; Shuh, D. K.; Tonner, B.; Tyliszczak, T.; Warwick, T.; Yoon, T. H. *J. Electron. Spectrosc. Relat. Phenom.* **2006**, *150*, 86-104.

(18) Because the gas is at room temperature and the surface is not, using the surface temperature to determine relative humidity is not strictly correct. However, since in equilibrium adsorption and desorption rates are the same, it is easy to see that it is the surface temperature that is important because it enters the desorption rate through an exponential $\exp(-E_a/RT)$, while the gas adsorption rate depends

on the collision rate, which depends on temperature as $T^{-1/2}$. The error in the RH committed by using T_{surf} is thus less than 7%.

(19) Yamamoto, S.; Andersson, K.; Bluhm, H.; Ketteler, G.; Starr, D. E.; Schiros, T.; Ogasawara, H.; Pettersson, L. G. M.; Salmeron, M.; Nilsson, A. *J. Phys. Chem. C* **2007**, *111*, 7848-7850.

(20) Andersson, K.; Ketteler, G.; Bluhm, H.; Yamamoto, S.; Ogasawara, H.; Pettersson, L. G. M.; Salmeron, M.; Nilsson, A. *J. Phys. Chem. C* **2007**, *111*, 14493-14499.

(21) First, the integrated intensity of each species at different H_2O pressure was normalized to the x-ray beam flux. The resultant values were then further normalized to the intensity of lattice oxygen of Cu_2O collected in UHV.

(22) Diebold, U. *Surf. Sci. Rep.* **2003**, *48*, 53-229.

(23) Brookes, I. M.; Muryn, C. A.; Thornton, G. *Phys. Rev. Lett.* **2001**, *87*, 266103.

(24) Wendt, S.; Matthiesen, J.; Schaub, R.; Vestergaard, E. K.; Laegsgaard, E.; Besenbacher, F.; Hammer, B. *Phys. Rev. Lett.* **2006**, *96*, 066107.

(25) Wendt, S.; Schaub, R.; Matthiesen, J.; Vestergaard, E. K.; Wahlstrom, E.; Rasmussen, M. D.; Thostrup, P.; Molina, L. M.; Laegsgaard, E.; Stensgaard, I.; Hammer, B.; Besenbacher, F. *Surf. Sci.* **2005**, *598*, 226-245.

(26) Liu, P.; Kendelewicz, T.; Brown, G. E.; Nelson, E. J.; Chambers, S. A. *Surf. Sci.* **1998**, *417*, 53-65.

(27) Bange, K.; Grider, D. E.; Madey, T. E.; Sass, J. K. *Surf. Sci.* **1984**, *137*, 38-64.

(28) Polak, M. *Surf. Sci.* **1994**, *321*, 249-260.

(29) Bange, K.; Madey, T. E.; Sass, J. K.; Stuve, E. M. *Surf. Sci.* **1987**, *183*, 334-362.

(30) Benndorf, C.; Madey, T. E. *Surf. Sci.* **1988**, *194*, 63-91.

(31) Clay, C.; Haq, S.; Hodgson, A. *Phys. Rev. Lett.* **2004**, *92*, 046102.

(32) Clay, C.; Haq, S.; Hodgson, A. *Chem. Phys. Lett.* **2004**, *388*, 89-93.

(33) Faradzhev, N. S.; Kostov, K. L.; Feulner, P.; Madey, T. E.; Menzel, D. *Chem. Phys. Lett.* **2005**, *415*, 165-171.

(34) Wagner, F. T.; Moylan, T. E. *Surf. Sci.* **1987**, *191*, 121-146.